NeuroImage 193 (2019) 25–34

Contents lists available at ScienceDirect

NeuroImage

journal homepage: www.elsevier.com/locate/neuroimage

Evidence for age-related changes in sensorimotor neuromagnetic responses during cued button pressing in a large open-access dataset

Timothy Bardouille [a,*], Lyam Bailey [b], CamCAN Group [c]

[a] Department of Physics and Atmospheric Science, Dalhousie University, Halifax, NS, Canada
[b] Department of Psychology and Neuroscience, Dalhousie University, Halifax, NS, Canada
[c] Cambridge Center for Ageing and Neuroscience, University of Cambridge, Cambridge, UK

A B S T R A C T

Mu, beta, and gamma rhythms increase and decrease in amplitude during movement. This event-related synchronization (ERS) and desynchronization (ERD) can be readily recorded non-invasively using magneto- and electro-encephalography (M/EEG). In addition, event-related potentials and fields (i.e., evoked responses) can be elucidated during movement. There is some evidence that the frequency, amplitude and latency of the movement-related ERS/ERD changes with ageing, however the evidence surrounding this topic comes mainly from studies in sample sizes on the order of tens of participants. The objective of this study was to examine a large open-access MEG dataset for age-related changes in movement-related ERS/ERD and evoked responses. MEG data acquired at the Cambridge Centre for Ageing and Neuroscience during cued button pressing was used from 567 participants between the ages of 18 and 88 years. The characteristics movement-related ERD/ERS and evoked responses were calculated for each individual participant. Based on linear regression analysis, significant relationships were found between participant age and some response characteristics, although the predictive value of these relationships was low. Specifically, we conclude that peak beta rebound frequency and amplitude decreased with age, peak beta suppression amplitude increased with age, movement-related gamma burst amplitude decreased with age, and peak motor-evoked response amplitude increased with age. Given our current understanding of the underlying mechanisms of these responses, our findings suggest the existence of age-related changes in the neurophysiology of thalamocortical loops and local circuitry in the primary somatosensory and motor cortices.

1. Introduction

1.1. Non-invasive imaging of movement-related cortical responses

Neuromagnetic and neuroelectric oscillatory signals have been recorded non-invasively from the brain for decades using magneto- and electro-encephalography (M/EEG). In the context of the sensorimotor system, there is a long history of evidence for the existence of brain rhythms occurring in frequencies from 8 to 90 Hz (Pfurtscheller, 2001; Pfurtscheller and Andrew, 1999; Pfurtscheller et al., 1994; Pfurtscheller et al., 2005; Brown et al., 1998; Cheyne et al., 2008; Gross et al., 2005; Jurkiewicz et al., 2006; Pfurtscheller et al., 1997; Pfurtscheller and Lopes da Silva, 1999; Hari et al., 1997; de Pasquale et al., 2010; Brookes et al., 2011). These rhythms each change in different ways due to movement and sensory afferent input, and likely have different neural generators.

Mu and beta rhythms can be readily recorded from the cortex approximately in the 8–15 Hz and 15–30 Hz ranges, respectively. These rhythms reduce in magnitude (with respect to a baseline interval prior to the event) following tactile stimulation (Gaetz and Cheyne, 2006), and just prior to and following actual voluntary or passive movements, or imagined movements (Jurkiewicz et al., 2006; Pfurtscheller et al., 1999; Pfurtscheller and Neuper, 1997; Parkkonen et al., 2015). Mu and beta rhythm reduction sustains for prolonged actual or imagined movements for up to several seconds (Kraeutner et al., 2014; Boe et al., 2014), and for tactile stimulation when attention to the stimulus is required (Bardouille et al., 2010). The phenomenon of reduced mu and beta rhythm magnitude, known as event-related desynchronization (ERD), is likely an indicator of increased local processing in the underlying cortex, leading to an interpretation that these rhythms are inhibitory "idling" signals (Pfurtscheller, 2001; Pfurtscheller and Lopes da Silva, 1999; Pfurtscheller et al., 1996a; Pfurtscheller et al., 1996b). Others have suggested that this oscillatory activity may also be involved in maintaining the current sensorimotor state (Engel and Fries, 2010). Mu and beta rhythm suppression have been localized to both primary motor and somatosensory cortex (M1/S1), with some evidence for a somatotopic representation (Pfurtscheller et al., 1997; Hari et al., 1997; Crone et al., 1998).

Roughly 500 ms following stimulus offset or the completion of an actual voluntary or passive movement, or imagined movement, the beta rhythm increases in magnitude with respect to a baseline period preceding the event (Pfurtscheller et al., 1996a, 2005; Parkkonen et al., 2015; Boe et al., 2014; Bardouille et al., 2010). By approximately 1–2 s following offset, the beta rhythm settles back to its original magnitude,

* Corresponding author.
E-mail address: tim.bardouille@dal.ca (T. Bardouille).

https://doi.org/10.1016/j.neuroimage.2019.02.065
Received 31 October 2018; Received in revised form 24 February 2019; Accepted 25 February 2019
Available online 5 March 2019

with differences in latency depending on task/stimulus (Houdayer et al., 2006). This period of ERS is often termed the post-movement beta rebound (PMBR). The localization of the beta rebound is typically more anterior than beta suppression, suggesting a likely M1 generator (Jurkiewicz et al., 2006). Both suppression and rebound tend to be bilateral responses, with dominance for contralateral responses for a stimulus/task in unilateral paradigms. Inter-hemispheric phase difference between the rhythms bilaterally indicates separate underlying generators (Andrew and Pfurtscheller, 1999). Beta suppression and rebound have also been reported bilaterally at secondary somatosensory cortex (Della Penna et al., 2004) and in the subthalamic nucleus (Kuhn, 2004). The mu and beta rhythms are thought to be the results of synchronized activity in thalamocortical neuronal loops (Pfurtscheller and Lopes da Silva, 1999). There is currently no evidence for a post-movement ERS in the mu frequency band, which suggests different mechanisms for the mu and beta rhythms.

A burst of ERS has been noted in the 60–90 Hz frequency range (i.e., gamma band) during simple, transient unilateral voluntary movements (Cheyne et al., 2008; Cheyne and Ferrari, 2013; Muthukumaraswamy, 2011). The movement-related gamma burst (MRGB) generally occurs over a duration of a few hundred milliseconds temporally centered at the time of the movement. The gamma band ERS is strongly lateralized to the hemisphere contralateral to movement, and localizes focally to MI with a somatotopic representation (Pfurtscheller et al., 1994; Cheyne et al., 2008). The movement-related gamma burst has been reported mainly at cortical sites via invasive recordings, and is thought to have an excitatory functional role in monitoring and generating movement (Szurhaj et al., 2006).

In addition to the oscillatory correlates of sensorimotor activity, MEG and EEG have been used to investigate patterns of average movement-evoked neural responses. In MEG, the strongest and most reliable of such motor-evoked fields is the MEF1, which typically onsets around 30–50 ms following a voluntary or passive movement (Cheyne and Weinberg, 1989; Kristeva et al., 1991; Kristeva-Feige et al., 1995; Lange et al., 2001), and is generally thought to reflect the proprioceptive signal arising from the moving limb (Kristeva-Feige et al., 1995; Cheyne et al., 2006). The MEF1 is typically localized to the contralateral central sulcus (Kristeva-Feige et al., 1995; Lange et al., 2001; Nagamine et al., 1996; Woldag et al., 2003), although some reports disagree over the relative contributions of its anterior and posterior banks (Kristeva-Feige et al., 1995; Cheyne et al., 2006; Woldag et al., 2003; Oishi et al., 2004; Ganslandt et al., 1999).

1.2. Movement-related responses and ageing

Age-related changes in cortical oscillations have been reported in the past (e.g. (Rossini et al., 2007),). Changes in cortical rhythm frequency and amplitude have been linked to resting concentration of the inhibitory neurotransmitter γ-Aminobutyric acid (GABA), suggesting a potential underlying mechanism (Gaetz et al., 2011; Muthukumaraswamy et al., 2013). For example, a reduction in amplitude of the beta rebound with increasing age (as compared to young adults) has been reported in a number of tasks (Babiloni et al., 2004; Labyt et al., 2003; Schmiedt-Fehr et al., 2016; Christov and Dushanova, 2016; Sallard et al., 2016; Toledo et al., 2016a). At the other end of the ageing spectrum, children demonstrate a reduced rebound amplitude during simple voluntary button pressing, as compared to young adults (Gaetz et al., 2010). Prolonged and reduced asymmetry in mu and beta suppression with ageing have also been reported (Labyt et al., 2003; Vallesi et al., 2010), as well as an increase in baseline beta signal power in M1 contralateral to a unilateral voluntary movement (Rossiter et al., 2014; Heinrichs-Graham and Wilson, 2016). In data recorded during simple movements, older participants exhibited a decrease in the frequency of beta suppression (Rossiter et al., 2014). There is also some evidence for a decrease in the frequency of the gamma burst with ageing, based on data spanning a limited number of years (Cheyne and Ferrari, 2013; Gaetz et al., 2011).

Age-related changes in the temporal and spatial characteristics of motor-evoked fields and potentials have received relatively little scientific attention, though some findings to date have indicated a perturbative role of ageing on motor-evoked responses. For example, the magnitude of positive-going deflections in the event-related potential immediately following a forced-choice motor response was diminished in older adults compared to young (Yordanova et al., 2004), although this difference did not extend to a simple cued finger-tapping task. Moreover, negative-going evoked potentials previously associated with proprioceptive feedback (Alary et al., 1998) exhibited significantly diminished amplitude and longer latency following both voluntary and passive movements in older, compared to younger adults (Toledo et al., 2016b). More recently, older adults were shown to exhibit stronger cortico-kinematic coherence (CKC) – a quantified metric of coupling between passive or active movement kinematics and associated neural activity (in this case measured with MEG) (Jerbi et al., 2007; Bourguignon et al., 2011; Piitulainen et al., 2013) – relative to younger adults following passive ankle movements; while these groups did not differ in peak-to-peak amplitude of the motor-evoked response (Piitulainen et al., 2018). On the other end of the age spectrum, a delayed MEF1 in children aged 3–5 years, occurring 140 ms post-movement – around 100 ms later than is typically observed in adults – has been reported, which the authors attributed to underdeveloped proprioceptive processing (Cheyne et al., 2014). It is worth noting that many of the studies cited above reported remarkably low variance in the temporal and spatial characteristics of post-movement evoked responses between individual participants, indicating a minimal influence of individual differences such as age. In a separate vein, work with fMRI has indicated greater activation in contralateral motor cortices in young, relative to elderly adults following a simple finger-tapping task (Hutchinson et al., 2002), while this relationship appears to be reversed in contralateral somatosensory cortex (Mattay et al., 2002).

Overall, the relationship between age and movement-evoked neural activity remains unclear. Evidence from EEG supports the view that ageing may perturb neural correlates of motor actions resulting in diminished responses with longer latencies. However, it is unclear if this is more related to complex motor planning than to simple voluntary movement. Results from fMRI suggest mixed age-related changes in the magnitude of motor-related responses, but are not informative as to the underlying electrophysiology. As such, further work is needed to clarify potential age-related changes in the electrophysiological correlates of voluntary movement.

1.3. Open-access imaging datasets

Recently, there has been a trend toward acquiring large neuroimaging datasets, with the purpose of making these so-called “open-access” data available to researchers outside of the team acquiring the data. Some examples include the Human Connectome Project (Van Essen et al., 2013) and the Cambridge Centre for Ageing and Neuroscience (Cam-CAN) (Shafto et al., 2014; Taylor et al., 2017) datasets. Of particular interest for this paper is the Cam-CAN dataset, which is a “comprehensive and theoretically-motivated examination of the hypothesis that preserved cognition across the lifespan depends on the brain remaining functionally flexible”. This particular dataset contains demographic, behavioural, and neuroimaging data. Specifically, the dataset includes MEG and structural/functional magnetic resonance imaging (MRI/fMRI) data for roughly 700 participants. An interesting component of this dataset is that the sample has a uniform distribution of participants between the ages of 18 and 88 years.

The Cam-CAN dataset includes MEG data obtained during the performance of a simple cued-button pressing task. We were interested to examine this large dataset to investigate age-related changes in the movement-related responses measured with MEG.

1.4. Objectives and hypotheses

The objective of this study was to examine MEG data during a simple button-press task from the Cam-CAN dataset for age-related changes in known neuroelectrophysiological responses occurring during movement. Based on previous literature, we hypothesized that there would be a positive correlation between increasing age and (1) decreasing beta rebound amplitude, (2) decreasing beta rebound peak frequency, (3) decreasing beta suppression frequency, and (4) decreasing gamma burst frequency. Given the stability of the MEF1 characteristics during simple voluntary motor paradigms in prior work, we hypothesized that there would be no correlation between age and MEF1 latency or amplitude.

2. Materials and methods

2.1. Participants and experimental paradigm

A total of 708 participants were recruited into Phase 2 of the Cam-CAN examination of healthy cognitive ageing. Of these 708 participants, 650 (91.8%) had MEG data obtained during the performance of the simple cued-button pressing task. Participant ages ranged from 18 to 88 years of age, with recruitment targeted to provide equal distribution in age per decile and equal proportions of males and females. Following exclusions (described in the analysis section), we report findings from 567 participants (80.1% of the original 708 participants).

In the Cam-CAN Phase 2 MEG session, each participant performed the "Sensorimotor task" (Shafto et al., 2014), in which participants responded with a right index finger button press to unimodal or bimodal audio/visual stimuli. The audio stimuli were binaural pure tones of 300-ms duration at a frequency of 300, 600, or 1200 Hz. The visual stimuli were checkerboards presented both to the left and right of a central fixation for 34-ms duration. Participants first completed a practice trial, followed by 128 trials in which 120 had bimodal stimulation, and 8 had unimodal stimulation. The order of bimodal and unimodal trials was randomized, and the inter-trial interval varied between 2 and 26 s.

2.2. Data acquisition

As indicated above, data used in the preparation of this work were obtained from the Cam-CAN repository (available at http://www.mrc-cbu.cam.ac.uk/datasets/camcan/) (Shafto et al., 2014; Taylor et al., 2017). MEG data were acquired at 1000 Hz with inline band-pass filtering between 0.03 and 330 Hz using a 306-channel Vectorview system (Elekta Neuromag, Helsinki, Finland). Digitization of anatomical landmarks (i.e., fiducial points; nasion and left/right preauricular point) as well as additional points on the scalp was also performed for registration of MEG and MRI coordinate systems. Head position was monitored continuously, and electrooculogram (EOG) and electrocardiogram (ECG) were recorded concurrently along with stimulus/response event markers. T1-weighted magnetic resonance images (MRI) were acquired using the 3T Siemens Tim Trio system with a 32-channel head coil.

2.3. MRI data analysis

For each participant, reconstruction was performed on the structural T1-weighted MRI using the FreeSurfer recon-all algorithm (Dale et al., 1999; Fischl and Dale, 2000; Fischl et al., 1999a, 1999b, 2001, 2002, 2004; Desikan et al., 2006). Importantly, this process provided a reconstruction of the cortical surface for source estimation, and a transformation to an average brain (i.e., fsaverage) for spatial normalization and group statistics. A boundary element model of the brain was also generated to provide more accurate calculation of the forward solution (Hamalainen and Sarvas, 1989), and a "source space" grid was defined on the cortical surface with 5 mm spacing as locations for source estimation. Finally, each participant's MRI data was registered to the MEG data based on the alignment of anatomical landmarks (i.e., fiducials) in MEG and MRI, and MEG head digitization with the scalp as visualized on the MRI (MNE python coreg, v.0.14). Datasets were aligned by a semi-automated procedure. The fiducial points were manually identified on the MRI, and the MEG-digitized fiducials were automatically translated and rotated (no scaling) to minimize the fiducial registration error between MEG and MRI points. Finally, manual translation and rotation was performed to improve alignment of the MEG-digitized additional points with the scalp, while maintaining FRE on the order of 0.5 cm.

2.4. MEG pre-processing – sensor level data

Data was pre-processed by the Cam-CAN group using temporal signal space separation to perform environmental noise reduction, reconstruction of missing or corrupted MEG channels, continuous head motion correction, and a transform of each dataset to a common head position (Taulu and Simola, 2006). All subsequent MEG processing was completed in the Python programming environment (v.2.7.13), using the MNE-python library (v.0.16.1) (Gramfort et al., 2014).

Raw MEG data were low-pass filtered at 125 Hz and notch filtered at 50 Hz and 100 Hz to remove signals related to power lines. Following this, the latency of each button-press was determined from the event markers encoded in the MEG data file, and the data was parsed into epochs synchronized to each button press. Each epoch had a duration of 3.4 s, with a 1.7 s pre-stimulus interval. Epochs were excluded if the button press occurred more than 1 s after the cue (indicating poor task performance) or if the button press occurred within 3 s of the previous button press (which provided insufficient baseline for subsequent analysis). Participants with less than 59 epochs after these exclusions were excluded from further analysis (57 participants).

Independent component analysis was performed on the epoched data using the FASTICA algorithm (Hyvarinen et al., 2010) to remove artifacts using a fully automated process. Briefly, the MEG data were decomposed into independent components (Delorme et al., 2007). Epochs with signals that exceeded 5 pT (magnetometers) or 400 pT/cm (gradiometers) were not included when calculating the deconstruction. Following this, components were excluded if the amplitude and phase of the component was similar to that of the EOG or ECG (Dammers et al., 2008). Finally, the MEG sensor data was reconstructed from the remaining components. This process resulted in cleaned MEG epoch data (i.e., channels x time x epochs), which were used for source estimation and time-frequency analysis. Finally, an inter-trial average was generated per participant to observe the motor evoked field (i.e., channels x time). Grand-average motor evoked field data was also generated by averaging the motor event-related field (ERF) data across all participants.

2.5. Time-frequency analysis – wide band

For each participant's epoched data, a Morlet wavelet analysis was completed to generate time-frequency response (TFR) plots that investigate movement-related signal power changes as a function of time and frequency. The evoked response was subtracted from each epoch prior to wavelet analysis to attenuate phase-locked changes in the data. Morlet wavelet analysis was performed at frequencies between 5 and 90 Hz with a 5 Hz step to estimate signal power over time for each epoch, and results were averaged across epochs to generate the final TFR (i.e., channels x time x frequency). The wavelet number of cycles was set to one half of the frequency, and data were decimated by a factor of 3 (to 333 Hz) to increase processing speed and reduce disk usage. For each TFR and frequency bin, the baseline signal power was calculated as the mean signal power between −1.5 and −1.0 s with respect to the button press. Following this, each value in the TFR was recalculated as the logarithm (base-10) of the ratio between the value and the baseline signal power. The logarithm of ratio power change was used as the measure of ERS/ERD. Thus, negative and positive values indicated a decrease (ERD) or increase (ERS) in signal power, respectively. Grand-average TFRs were also generated by averaging the ERS/ERD result across participants.

2.6. Localizing oscillatory responses

For each participant, dynamic imaging of coherent sources (Gross et al., 2001) was used to localize the generator of the beta suppression during movement, beta rebound, and gamma burst by beamforming to the source space on the cortical surface. Based on the grand-average ERS/ERD results, the active time interval for beta rebound beamforming was 500–1250 ms following the button press, the baseline interval was 250–1000 ms prior to the button press, and the frequency band of interest was 15–30 Hz. For the beta suppression, the active time interval for beamforming was −100 to 500 ms following the button press, the baseline interval was 400–1000 ms prior to the button press, and the frequency band of interest was 15–30 Hz. For the gamma burst, the active time interval for beamforming was −200 to 200 ms following the button press, the baseline interval was 600–1000 ms prior to the button press, and the frequency band of interest was 65–95 Hz. The boundary element model was used for more accurate modelling of the magnetic field, compared to a spherical model. The resultant maps were spatially normalized to the spherically-aligned *fsaverage* template brain to enable group statistics (Fischl et al., 1999b). A grand-average map was also generated for each response by averaging the spatially normalized maps across participants.

A functional region of interest (ROI) for the group was generated for each ERS/ERD response as a spatial mask for estimating time-frequency characteristics of that response on a single-subject basis. To define the functional ROI, a mask was generated for each participant's spatially normalized map such that the top 5% of values were set to a value of one and all other vertices were set to zero. A cumulative map was generated by summing the masks across all participants. A threshold was then applied to the cumulative map, and the largest cluster in the thresholded image defined the functional ROI. For the beta suppression and rebound, the threshold applied to the cumulative map was 50% of participants. For the gamma burst, the threshold applied to the cumulative map was 20% of participants. Percentage thresholds were determined manually to provide a single contiguous functional ROI in the contralateral hemisphere for each response, and differed due to the distribution and spatial smoothness of each map. For all three responses, this process resulted in an ROI that was proximal to the left central sulcus. The functional ROI, defined in the template brain space, was then transformed back into each participant's original MRI coordinate frame. The centre of mass (CoM) of the ROI was then determined and used as the target location for time-frequency analysis of brain activity, as described below.

2.7. Time-frequency analysis – finding rhythm characteristics

For each participant, the time course of activity at the target location (i.e., CoM of the functional ROI) was estimated using the beamformer spatial filter applied to the cleaned MEG epoch data. A TFR plot was generated at the target location based on this time course. For the beta suppression and rebound, the new TFR had a frequency resolution of 1 Hz between 10 and 35 Hz, and a temporal window of 3 s centered on the button press. For the gamma burst, the new TFR had a frequency resolution of 1 Hz between 60 and 95 Hz, and the same temporal window. As above, ERS/ERD was estimated by normalizing to a baseline interval occurring 1.0–1.5 s prior to the button press. For each response and each participant, the frequency, amplitude, and latency of the global maximum in the active time window (defined above for beamforming) was identified and recorded as input data to the group-level age-related analysis. For the beta suppression response, the global minimum was used instead of the global maximum.

2.8. Localizing the event-related field

Similar to the ERS/ERD localization, generators of the ERF data for each participant were estimated by beamforming to the source space on the cortical surface. The cleaned MEG epochs, after applying a low-pass filter at 40 Hz and downsampling to 200 Hz, were used for generating event-related beamformer (ERB) maps. Based on the grand-average motor ERF, the active time interval for beamforming was chosen as −200 to 300 ms relative to the button press, and the baseline interval was 500–1000 ms prior to the button press. Each resultant ERB map was transformed to match the template brain, and a grand-average ERB map was generated by averaging the spatially normalized maps across participants. The grand-average ERB data indicated a peak in activity in contralateral M1 at 50 ms following the button press, as expected for the MEF1.

The functional ROI was generated as a spatial mask for estimating temporal characteristics of the ERF at the individual-subject level. Given the peak in activity at 50 ms in the grand-average ERB map, each participant's ERB map was averaged across time between 35 and 65 ms, to generate an activation map per participant that was specific to the MEF1. An ROI was defined that included all vertices that were in the top 5% of values in this activation map for more than 10% of participants. The resultant ROI included bilateral activation of primary sensorimotor cortices, as well as areas near the sylvian fissure. Thus, the functional ROI was further constrained to include only those vertices that overlaid the contralateral central sulcus and the pre- and post-central gyri, as labelled by the FreeSurfer 'aparc' reconstruction (Desikan et al., 2006). The functional ROI was then transformed back into each participant's native MRI coordinate frame, and the CoM extracted for each participant. The time course of estimated ERB source activity at the CoM was used to characterize the event-related brain activity at the individual-subject level, as described below.

2.9. Finding event-related characteristics

For each participant, the time course of activity at the target location associated with the ERF was constrained to a user-defined time window of −100 to 250 ms relative to the button press, based on visual inspection of the grand-average data. From this time course, the latency and amplitude of the strongest local maximum (i.e., peak amplitude), along with the average amplitude over the 35–65 ms time window, were recorded as input data to the group-level analysis.

2.10. Statistical analysis

For group-level analysis, linear regression was used to reveal significant relationships between age and changes in the ERS/ERD response peak frequency, amplitude and latency, as well as changes in the amplitude and latency of the event-related response ($p < 0.05$).

2.11. Data and code availability

All determined MRI-MEG co-registration files for the CamCAN dataset are available at (https://github.com/tbardouille/camcan_coreg). MEG data analysis scripts are available at (https://github.com/tbardouille/camcan_MovementInducedResponses).

3. Results

3.1. Behavioural data

3.1.1. Demographics

Of the 650 participants with MEG data for the button press task, 57 (8.8%) were excluded from the statistical analysis because there was insufficient MEG data after applying trial exclusions described above. Of the remaining participants, 22 (3.7%) were excluded due to issues during the FreeSurfer recon-all process, and four (0.6%) were excluded due to issues arising during the beamforming process (e.g., singular value decomposition did not converge). Thus, statistical analysis was performed on 567 participants. During pre-processing, 3.4 ± 1.0 independent components were removed from each dataset and 62.7 ± 0.8 button

press events were included in the analysis for each participant.

As shown in Fig. 1, the CamCAN dataset and the subset of participants included in the results of this manuscript demonstrate a uniform distribution of age between 18 and 88 years for both male and female participants. The distribution of handedness indicates that the majority of participants were right hand dominant. Across all participants, the mean response time between the cue and the button press was 303 ± 64 ms (mean ± standard deviation). The results of a linear regression indicated that there was no significant relationship between response time and age ($p > 0.05$).

3.2. Movement-related time-frequency responses

Fig. 2 shows the grand-average TFR plot for a left-central MEG sensor (MEG0711) that indicates patterns of ERS/ERD observed with respect to the button press. The beta suppression begins just prior to the button press, and has a duration of roughly 600 ms. The rebound occurs 500–1250 ms following the button press. Both the suppression and rebound are maximal in the 15–30 Hz frequency range. Mu rhythm suppression is also apparent. As expected, there is no rebound associated with the mu rhythm. The gamma burst can be observed in an interval 200 ms prior to and following the button press in the 65–95Hz frequency range, although this response is small in magnitude.

Fig. 3 shows the grand-average localization of the beta suppression, beta rebound, and gamma burst. The beta suppression localizes to bilateral primary motor and somatosensory cortices, with a clear contralateral dominance. While the beta suppression shows equivalent activation of primary motor and somatosensory cortex, the rebound has a more anterior pattern, which is focused on the pre-central gyrus. The rebound also shows a more medial localization compared to the beta suppression. The gamma burst map indicates dominant activation in contralateral primary motor cortex, with some activation of the contralateral primary somatosensory cortex and bilateral occipital lobes. Functional ROIs for extracting the time courses for all responses, as shown in Fig. 3, are specific to the primary somatosensory and motor cortices in the contralateral hemisphere.

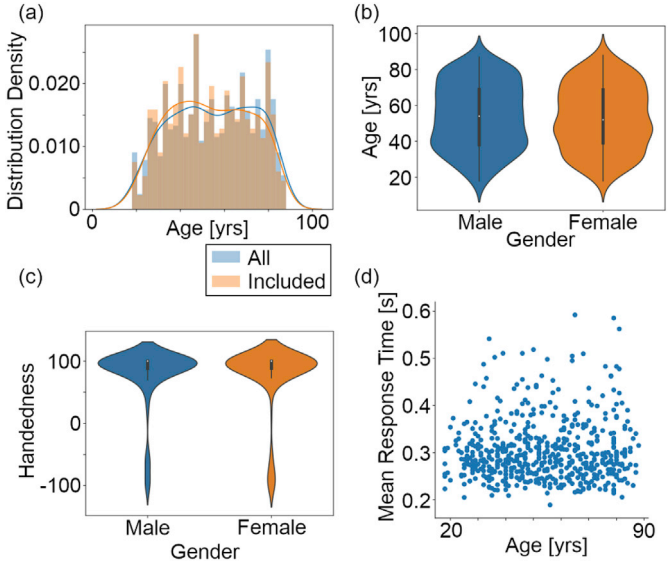

Fig. 1. Demographic data for participants from the Cam-CAN open-access dataset. (a) Histogram of participant age before (blue) and after (green) exclusion. (b) Violin plots of age distribution separately for males (blue) and females (green). (c) Violin plots of handedness separately for males (blue) and females (green). (d) Scatter plot of mean button press response time per participant as a function of age.

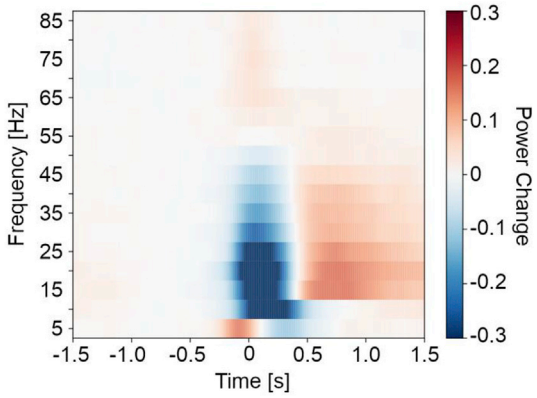

Fig. 2. Grand-average time-frequency response (TFR) plot of the induced response to cued button press at a left-central sensor (MEG0711). Beta and mu event-related desynchronization (ERD) are evident in the TFRs, as well as beta rebound following the ERD and gamma event-related synchronization at the time of the button press.

3.3. Movement evoked response

The grand-averaged movement evoked field (MEF) is shown in Fig. 4a. Large amplitude field deflections are present at −100, 50, and 125 ms, with bilateral dipolar patterns likely represented at 50 ms. The grand-average ERB map at 50 ms (Fig. 4b) clearly shows bilateral activation of primary motor and somatosensory cortices at locations typically associated with the somatotopic representation of the hand, which is in keeping with expectations for a cued right-handed button press. Given that the mean response time was 303 ms, activation observed in areas near the sylvian fissure at 50 ms post-button press may represent cortical responses to the 300-ms duration auditory component of the cue. The functional ROI for extracting the time course of the evoked response, as shown in Fig. 4c, overlaps the central sulcus contralateral to the hand making the button press. The location is consistent with expectations for the somatotopic representation of the hand.

3.4. Response attributes by age

Individual participant's data were used to identify the peak frequency, amplitude and latency of the beta suppression, beta rebound and gamma burst, and peak (and mean) amplitude and latency of the MEF1. Fig. 5 shows each response characteristic as a function of age for all participants, including a linear regression line with 95% confidence interval indicated (shaded region). There is evidence for an age-related increase in the amplitude of the beta suppression and the MEFI. An age-related decrease is evident in the beta rebound frequency and amplitude, and the gamma burst amplitude. Table 1 tabulates changes in response characteristics with age for the beta suppression, beta rebound, gamma burst and MEF1. As hypothesized, significant regression equations were found between age and beta rebound amplitude, and between age and rebound frequency. A significant regression equation was found to predict peak beta rebound amplitude based on age ($p < 0.05$), with an R^2 of 0.0092. Participant's predicted beta rebound peak amplitude is equal to 0.161–0.000314 (age), when age is measured in years. Thus, participant's rebound peak amplitude decreased with increasing age. A significant regression equation was found to predict peak rebound frequency based on age ($p < 0.05$), with an R^2 of 0.0097. Participant's predicted rebound peak frequency is equal to 21.2 Hz–0.037 Hz (age), when age is measured in years. Thus, participant's rebound peak frequency decreased by 0.037 Hz for each year of age. The predictive value of these relationships is low, given the reported R^2 values. Contrary to our hypotheses, there was a significant positive correlation between age and peak amplitude of the MEF1 ($p < 0.05$, $R^2 = 0.0074$), however no significant relationships were observed with respect to average amplitude or latency ($p > 0.05$ in

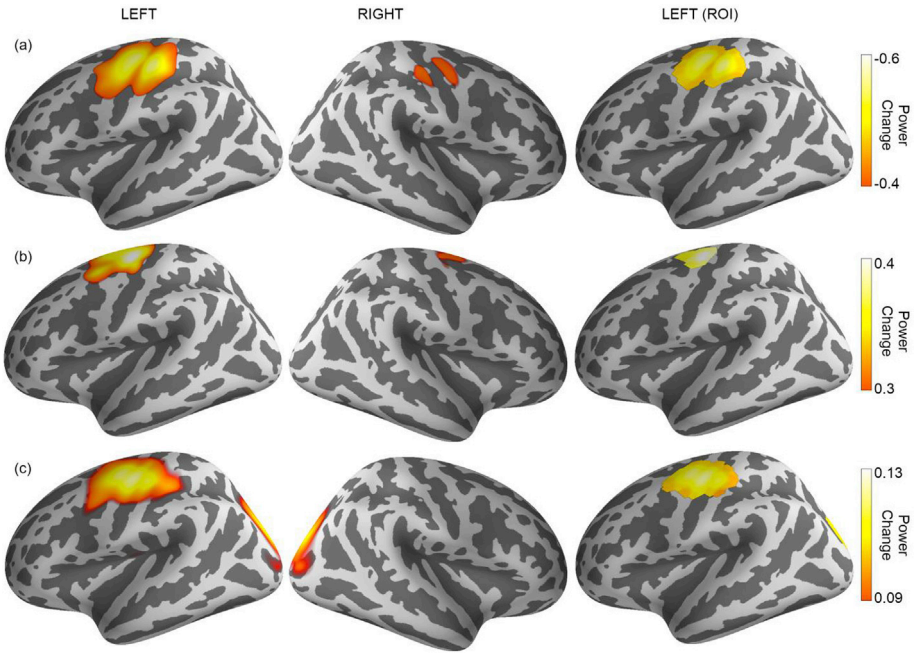

Fig. 3. Beamformer maps averaged across all participants are shown for (a) beta event-related desynchronization, (b) post-movement beta rebound, and (c) movement-related gamma burst. Grand-average maps are shown for the left and right hemispheres (left and middle columns). The functional region of interest used for estimating response characteristics is shown in the right column.

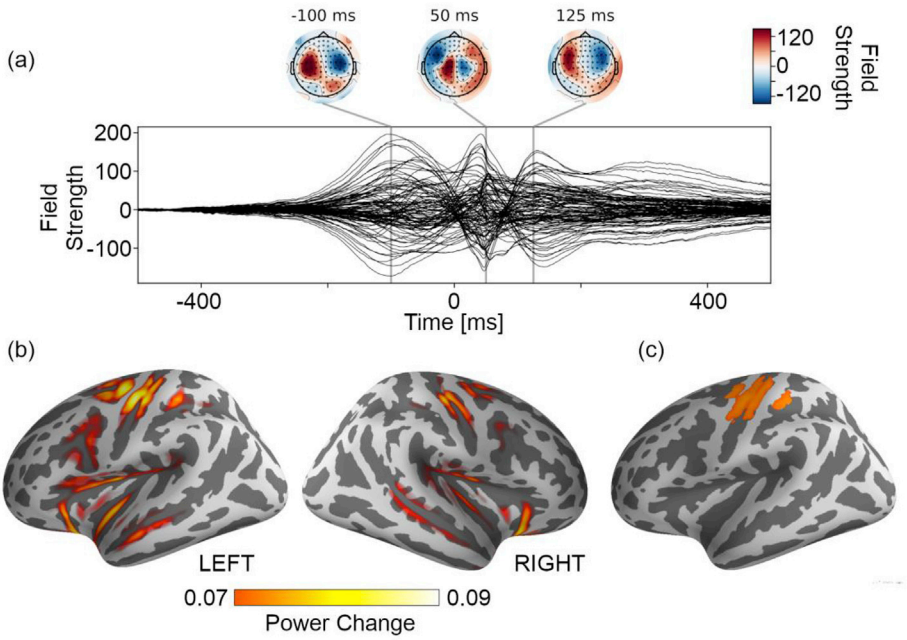

Fig. 4. Grand-average motor evoked response data is shown. (a) A butterfly plot showing an overlay of grand-average magnetic field deflections for 102 magnetometers (gradiometer data are not shown). The onset of the cued button press occurs at t = 0 s. Contour representations of the field topographies at peak latencies are also shown. (b) The beamformer map averaged across all participants for the 50 ms response are shown for the left and right hemispheres. (c) The functional region of interest used for estimating response characteristics is shown.

both cases). Finally, contrary to our hypotheses there was no significant relationship between age and beta suppression frequency, or between age and gamma burst frequency.

Exploring other response characteristics, we found a strong relationship between age and beta suppression amplitude. A significant regression equation was found to predict peak suppression amplitude based on age ($p < 0.05$), with an R^2 of 0.064. Participant's predicted suppression peak amplitude is equal to 0.121 + 0.000914 (age), when age is measured in years. Thus, participant's beta suppression peak amplitude increased (i.e., stronger desynchronization) with increasing age. We also found a relationship between age and gamma burst amplitude. A significant regression equation was found to predict peak gamma burst amplitude based on age ($p < 0.05$), with an R^2 of 0.015. Participant's predicted gamma burst peak amplitude is equal to 0.0832–0.000191 (age), when age is measured in years. Thus, participant's gamma burst peak amplitude decreased (i.e., weaker synchronization) with increasing age.

4. Discussion

This study reports on age-related changes in the cortical oscillations and evoked responses during cued button pressing in a population one

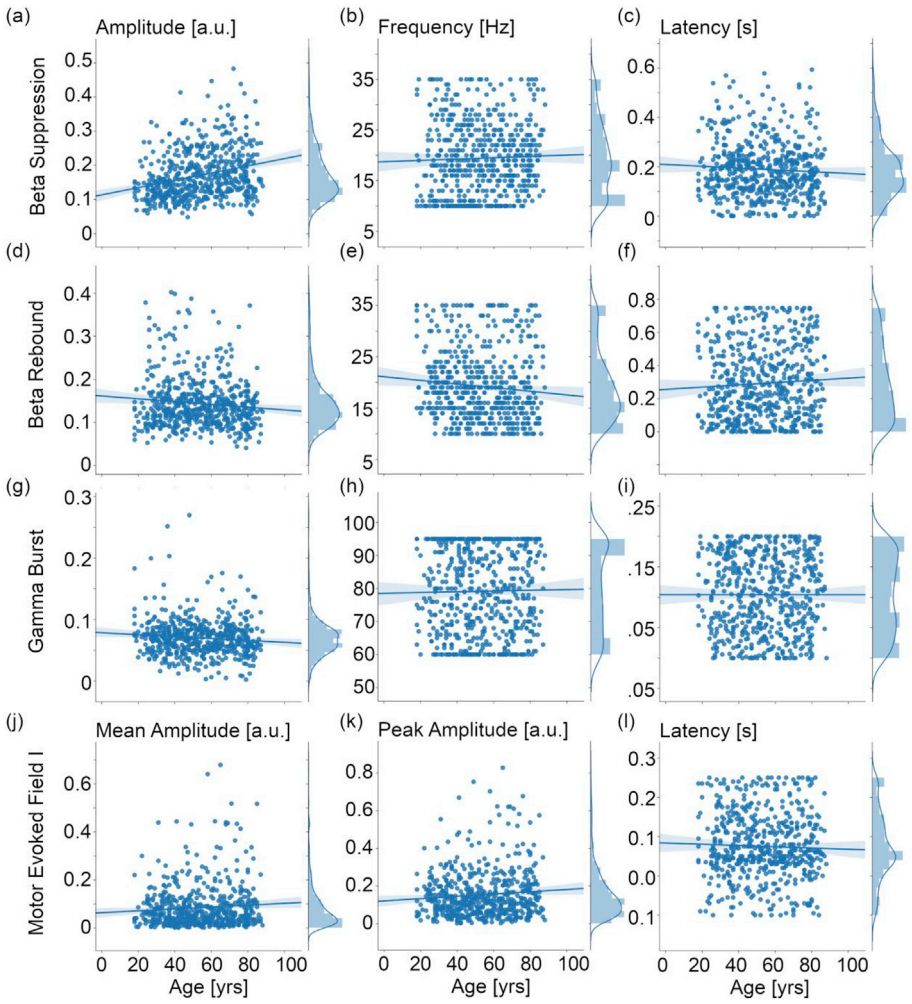

Fig. 5. Scatter plots of the age-related change in each response characteristic. Each point indicates the value of the response characteristic for a single participant for the beta suppression during movement (a–c), post-movement beta rebound (d–f), movement-related gamma burst (g–i), and the motor evoked field (j–l). The solid line indicates the linear regression, with the 95% confidence interval indicated by the shaded regions.

Table 1
Response Characteristics vs. Age Regression Results.

Response	Characteristic	Intercept	Slope	*p*	R^2
PMBR	**Frequency**	**21.2 Hz**	**−0.0370 Hz**	**0.018**	**0.0097**
PMBR	**Amplitude**	**0.161**	**−0.000314**	**0.022**	**0.0092**
PMBR	Latency	759 ms	0.611 ms	0.24	0.0024
ERD	Frequency	17.7 Hz	0.0195 Hz	0.22	0.0026
ERD	**Amplitude**	**0.121**	**0.000914**	**1.1 e-9**	**0.064**
ERD	Latency	127 ms	−0.524 ms	0.054	0.0065
MRGB	Frequency	77.3 Hz	0.00206 Hz	0.94	8.5e-6
MRGB	**Amplitude**	**0.0832**	**−0.000191**	**0.0037**	**0.015**
MRGB	Latency	−97.9 ms	0.0191 ms	0.94	1.1e-5
MEF1	**Peak Amplitude**	**0.121**	**0.00605**	**0.03**	**0.0074**
MEF1	Average Amplitude	0.063	0.000392	0.06	0.0059
MEF1	Latency	84.0 ms	−0.159 ms	0.42	0.0011

order of magnitude larger than previous studies. The substantial increase in sample size, thanks to the team behind the Cam-CAN dataset, provides definitive findings compared to previous studies. The changing characteristics of the oscillatory responses with age have important implications for neuroimaging studies focused on the sensorimotor network. The beta suppression and rebound are thought to be correlates of changes in synchronized activity in a thalamocortical neuronal loop (Pfurtscheller and Lopes da Silva, 1999). Given the results provided here, it is clear that the behavior of this neuronal loop changes with age, as evidenced by changes in response amplitude and frequency. Despite considerable work examining the beta suppression and rebound in the context of ageing, the implications of these changes in terms of motor function are not well understood. Further work is required to understand the neural mechanisms and functional repercussions of the changes in these responses.

Regardless of the mechanism underlying the changes, the findings of our study make it clear that caution should be taken when extrapolating results from the significant number of imaging studies involving younger participants to older populations. For example, there is increasing interest in neurofeedback and brain-computer interface applications that utilize changes in the cortical rhythms (Boe et al., 2014; Gruzelier, 2014; Pfurtscheller and Solis-Escalante, 2009). Our findings question the universal applicability of neurofeedback algorithms developed in younger participants for use in older populations.

In terms of localization, our results confirm previous reports of a bilateral pattern for beta suppression and rebound with a contralateral dominance (Jurkiewicz et al., 2006), and a contralateral localization for the MEFI (Cheyne et al., 2006). As expected, we also found that the rebound localizes anterior to the beta suppression (Jurkiewicz et al., 2006), which has maxima over both primary motor and somatosensory cortices. We also found that the gamma burst occurred essentially exclusively in the contralateral hemisphere, in keeping with previous reports (Pfurtscheller et al., 1994; Cheyne et al., 2008). As such, our data suggest, in a large cohort, that these three responses have different generators. Furthermore, the age-related decrease in magnitude of the

beta rebound (ROI anterior to the central sulcus) and increase in magnitude of the beta suppression (ROI across both banks of the central sulcus) provides an electrophysiological explanation for the opposing age-related changes in M1 as compared to S1, which were previously reported in fMRI (Hutchinson et al., 2002; Mattay et al., 2002).

Contrary to our predictions, we observed a weak but significant positive correlation between age and peak amplitude of the MEF1 response. By contrast, previous work has generally indicated no effect of age on motor-evoked response amplitude following cued finger tapping (Heinrichs-Graham and Wilson, 2016) or passive proprioceptive stimulation (Piitulainen et al., 2018), although one study reported *diminished* response amplitude amongst older (compared to younger) adults following both active and passive movements (Alary et al., 1998). The cause of this discrepancy is likely related to statistical power. The prior results discussed above were obtained from markedly smaller samples ($n < 50$ in all cases) compared to ours ($n = 567$) and therefore, in all likelihood, lacked sufficient statistical power to reveal the relatively weak effect of age observed in our analyses.

It is worth mentioning that our results are somewhat consistent with the recent finding that older adults exhibit stronger corticokinematic coherence (CKC) during passive movement (Piitulainen et al., 2018). This finding was attributed to age-related declines in the efficiency of proprioceptive processing. More specifically, the authors suggest that age-related motor deterioration may hinder cortical proprioceptive processing, and that enhanced CKC represents a compensatory effort to resolve proprioceptive input following age-related sensorimotor deficits. While CKC is not fully analogous to the MEF1, a similar interpretation may be applied to our findings. The MEF1 is generally thought to reflect proprioceptive processing arising from the moving limb (Kristeva et al., 1991; Lange et al., 2001). One may argue that the observed age-related increase in MEF1 amplitude reflects a similar compensatory effort – likely involving a larger neuronal population – to overcome sensorimotor deficits amongst older adults.

One consideration here is that the enhanced CKC observed in previous work (Piitulainen et al., 2018) was elicited during *passive* movement, and therefore may not provide a strong basis for comparison with our results. This issue highlights the difficulty of drawing inferences about cortical processing of proprioceptive afference from voluntary movement paradigms. While it is likely an important component of voluntary movement, further work is required to disentangle afferent proprioceptive processing from other components of motor control. This problem is complicated by the fact that afferent proprioceptive processing likely differs between voluntary and passive movements (without such a distinction, the motor system could not differentiate between external perturbations and internally generated movements). As such, it is difficult to make claims about proprioceptive processing during voluntary movement based on observations from passive movement paradigms alone. Future research in this vein should involve a combination of passive and active movement tasks within the same individuals, in order to pinpoint differences in sensorimotor integration of voluntary movement versus external perturbations of the motor system.

Finally, we did not expect to observe a movement-related increase in the gamma rhythm magnitude (i.e., ERS) in the occipital lobe. Previous reports related to the movement-related gamma burst have focused on self-paced simple movements, and have not reported response components in the occipital lobe (Cheyne et al., 2008; Cheyne and Ferrari, 2013; Muthukumaraswamy, 2011). It is possible that the visual gamma ERS reported here may be related to the checkerboard nature of the visual stimuli, in line with previous work relating gamma activity to the perception of visual gratings (Herrmann et al., 2010; Muthukumaraswamy et al., 2009; Muthukumaraswamy and Singh, 2008). Further work is required to investigate the occipital gamma ERS. Similarly, the event-related beamformer map at 50 ms shows activation in temporal and frontal areas, as well as the bilateral primary motor and somatosensory areas that were the focus of this manuscript. Temporal activation may be related to the auditory component of the stimuli. The temporal, frontal and occipital activation will require further investigation to elucidate their relationship to the task. However, investigating the relevance of the temporal and frontal activation to the task at hand is beyond the scope of this manuscript.

To maintain a reasonable scope, the current manuscript focused on spectral and temporal changes in areas of the contralateral primary somatosensory and motor cortices. Our analysis targets the same regions of interest for all participants when measuring peak characteristics for cortical oscillations and evoked responses. However, it is possible that some change in the spatial representation of the responses may occur with ageing, and this effect would not be represented in our results. Further work is required to investigate age-related changes in response characteristics in other areas of the brain.

Given the large number of participant's data in this study, the authors utilized automated analysis techniques as much as possible. All analysis steps included procedures to write the standard output and standard error data, and meta-data from each step (e.g., number of independent components removed) to log files. Automation enables the analysis of massive datasets and eliminates some of the opportunities through which human intervention can bias the findings. On the other hand, the subtleties of human decision making are difficult to represent fully in computer code. For example, the identification of independent components that represented artifacts was completely automated, as well as the detection of response characteristics in the evoked and TFR data. Independent components labelled as “artifacts” manually may not exactly match those that would be selected by an expert user (Griffanti et al., 2017), and the sensitivity and specificity of the automatic approach, compared to expert manual selection, is not known. Similarly, automated simple peak detection can be problematic, in particular with noisy data. New approaches to artifact classification and peak detection based on machine learning and big data may have value to address this weakness of the automated approaches used here. Despite best efforts at automation, significant human processing time was still required for the MEG-MRI co-registration. These data are now available via open-access, which should enable further analysis of the Cam-CAN data.

5. Conclusion

Movement-related responses in contralateral primary motor and somatosensory cortex during a cued button press task exhibit changes in their characteristics with ageing in a healthy population of over 550 participants between the ages of 18 and 88. Specifically, the post-movement beta rebound decreases in amplitude and frequency with age, the beta suppression during movement increases in amplitude with age, the movement-related gamma burst decreases in amplitude with age, and MEF1 increases in amplitude with age. These findings clarify and expand our current understanding of the neuromagnetic properties of the healthy ageing brain.

Acknowledgements

The authors would like to acknowledge the hard-working individuals involved in the acquisition of the Cam-CAN dataset for their commitment to open-access data, and Lindsey Power for assistance with MEG-MRI co-registration on this large dataset.

References

Alary, F., et al., 1998. Event-related potentials elicited by passive movements in humans: characterization, source analysis, and comparison to fMRI. Neuroimage 8 (4), 377–390.

Andrew, C., Pfurtscheller, G., 1999. Lack of bilateral coherence of post-movement central beta oscillations in the human electroencephalogram. Neurosci. Lett. 273 (2), 89–92.

Babiloni, C., et al., 2004. Human cortical rhythms during visual delayed choice reaction time tasks. A high-resolution EEG study on normal aging. Behav. Brain Res. 153 (1), 261–271.

Bardouille, T., Picton, T.W., Ross, B., 2010. Attention modulates beta oscillations during prolonged tactile stimulation. Eur. J. Neurosci. 31 (4), 761–769.

Boe, S., et al., 2014. Laterality of brain activity during motor imagery is modulated by the provision of source level neurofeedback. Neuroimage 101, 159–167.
Bourguignon, M., et al., 2011. Functional motor-cortex mapping using corticokinematic coherence. Neuroimage 55 (4), 1475–1479.
Brookes, M.J., et al., 2011. Investigating the electrophysiological basis of resting state networks using magnetoencephalography. Proc. Natl. Acad. Sci. U. S. A. 108 (40), 16783–16788.
Brown, P., et al., 1998. Cortical correlate of the Piper rhythm in humans. J. Neurophysiol. 80 (6), 2911–2917.
Cheyne, D., Ferrari, P., 2013. MEG studies of motor cortex gamma oscillations: evidence for a gamma "fingerprint" in the brain? Front. Hum. Neurosci. 7, 575.
Cheyne, D., Weinberg, H., 1989. Neuromagnetic fields accompanying unilateral finger movements - pre-movement and movement-evoked fields. Exp. Brain Res. 78 (3), 604–612.
Cheyne, D., Bakhtazad, L., Gaetz, W., 2006. Spatiotemporal mapping of cortical activity accompanying voluntary movements using an event-related beamforming approach. Hum. Brain Mapp. 27 (3), 213–229.
Cheyne, D., et al., 2008. Self-paced movements induce high-frequency gamma oscillations in primary motor cortex. Neuroimage 42 (1), 332–342.
Cheyne, D., et al., 2014. Movement-related neuromagnetic fields in preschool age children. Hum. Brain Mapp. 35 (9), 4858–4875.
Christov, M., Dushanova, J., 2016. Functional correlates of brain aging: beta and gamma components of event-related band responses. Acta Neurobiol. Exp. 76 (2), 98–109.
Crone, N.E., et al., 1998. Functional mapping of human sensorimotor cortex with electrocorticographic spectral analysis. I. Alpha and beta event-related desynchronization. Brain 121 (Pt 12), 2271–2299.
Dale, A.M., Fischl, B., Sereno, M.I., 1999. Cortical surface-based analysis - I. Segmentation and surface reconstruction. Neuroimage 9 (2), 179–194.
Dammers, J., et al., 2008. Integration of amplitude and phase statistics for complete artifact removal in independent components of neuromagnetic recordings. IEEE Trans. Biomed. Eng. 55 (10), 2353–2362.
de Pasquale, F., et al., 2010. Temporal dynamics of spontaneous MEG activity in brain networks. Proc. Natl. Acad. Sci. U. S. A. 107 (13), 6040–6045.
Della Penna, S., et al., 2004. Temporal dynamics of alpha and beta rhythms in human SI and SII after galvanic median nerve stimulation. A MEG study. Neuroimage 22 (4), 1438–1446.
Delorme, A., Sejnowski, T., Makeig, S., 2007. Enhanced detection of artifacts in EEG data using higher-order statistics and independent component analysis. Neuroimage 34 (4), 1443–1449.
Desikan, R.S., et al., 2006. An automated labeling system for subdividing the human cerebral cortex on MRI scans into gyral based regions of interest. Neuroimage 31 (3), 968–980.
Engel, A.K., Fries, P., 2010. Beta-band oscillations–signalling the status quo? Curr. Opin. Neurobiol. 20 (2), 156–165.
Fischl, B., Dale, A.M., 2000. Measuring the thickness of the human cerebral cortex from magnetic resonance images. Proc. Natl. Acad. Sci. U.S.A. 97 (20), 11050–11055.
Fischl, B., Sereno, M.I., Dale, A.M., 1999. Cortical surface-based analysis - II: inflation, flattening, and a surface-based coordinate system. Neuroimage 9 (2), 195–207.
Fischl, B., et al., 1999. High-resolution intersubject averaging and a coordinate system for the cortical surface. Hum. Brain Mapp. 8 (4), 272–284.
Fischl, B., Liu, A., Dale, A.M., 2001. Automated manifold surgery: constructing geometrically accurate and topologically correct models of the human cerebral cortex. IEEE Trans. Med. Imaging 20 (1), 70–80.
Fischl, B., et al., 2002. Whole brain segmentation: automated labeling of neuroanatomical structures in the human brain. Neuron 33 (3), 341–355.
Fischl, B., et al., 2004. Automatically parcellating the human cerebral cortex. Cerebr. Cortex 14 (1), 11–22.
Gaetz, W., Cheyne, D., 2006. Localization of sensorimotor cortical rhythms induced by tactile stimulation using spatially filtered MEG. Neuroimage 30 (3), 899–908.
Gaetz, W., et al., 2010. Neuromagnetic imaging of movement-related cortical oscillations in children and adults: age predicts post-movement beta rebound. Neuroimage 51 (2), 792–807.
Gaetz, W., et al., 2011. Relating MEG measured motor cortical oscillations to resting gamma-aminobutyric acid (GABA) concentration. Neuroimage 55 (2), 616–621.
Ganslandt, O., et al., 1999. Functional neuronavigation with magnetoencephalography: outcome in 50 patients with lesions around the motor cortex. J. Neurosurg. 91 (1), 73–79.
Gramfort, A., et al., 2014. MNE software for processing MEG and EEG data. Neuroimage 86, 446–460.
Griffanti, L., et al., 2017. Hand classification of fMRI ICA noise components. Neuroimage 154, 188–205.
Gross, J., et al., 2001. Dynamic imaging of coherent sources: studying neural interactions in the human brain. Proc. Natl. Acad. Sci. U. S. A. 98 (2), 694–699.
Gross, J., et al., 2005. Task-dependent oscillations during unimanual and bimanual movements in the human primary motor cortex and SMA studied with magnetoencephalography. Neuroimage 26 (1), 91–98.
Gruzelier, J.H., 2014. EEG-neurofeedback for optimising performance. I: a review of cognitive and affective outcome in healthy participants. Neurosci. Biobehav. Rev. 44, 124–141.
Hamalainen, M.S., Sarvas, J., 1989. Realistic conductivity geometry model of the human head for interpretation of neuromagnetic data. IEEE Trans. Biomed. Eng. 36 (2), 165–171.
Hari, R., et al., 1997. Magnetoencephalographic cortical rhythms. Int. J. Psychophysiol. 26 (1–3), 51–62.
Heinrichs-Graham, E., Wilson, T.W., 2016. Is an absolute level of cortical beta suppression required for proper movement? Magnetoencephalographic evidence from healthy aging. Neuroimage 134, 514–521.
Herrmann, C.S., Frund, I., Lenz, D., 2010. Human gamma-band activity: a review on cognitive and behavioral correlates and network models. Neurosci. Biobehav. Rev. 34 (7), 981–992.
Houdayer, E., et al., 2006. Relationship between event-related beta synchronization and afferent inputs: analysis of finger movement and peripheral nerve stimulations. Clin. Neurophysiol. 117 (3), 628–636.
Hutchinson, S., et al., 2002. Age-related differences in movement representation. Neuroimage 17 (4), 1720–1728.
Hyvarinen, A., et al., 2010. Independent component analysis of short-time Fourier transforms for spontaneous EEG/MEG analysis. Neuroimage 49 (1), 257–271.
Jerbi, K., et al., 2007. Coherent neural representation of hand speed in humans revealed by MEG imaging. Proc. Natl. Acad. Sci. U. S. A. 104 (18), 7676–7681.
Jurkiewicz, M.T., et al., 2006. Post-movement beta rebound is generated in motor cortex: evidence from neuromagnetic recordings. Neuroimage 32 (3), 1281–1289.
Kraeutner, S., et al., 2014. Motor imagery-based brain activity parallels that of motor execution: evidence from magnetic source imaging of cortical oscillations. Brain Res. 1588, 81–91.
Kristeva, R., Cheyne, D., Deecke, L., 1991. Neuromagnetic fields accompanying unilateral and bilateral voluntary movements: topography and analysis of cortical sources. Electroencephalogr. Clin. Neurophysiol. 81 (4), 284–298.
Kristeva-Feige, R., et al., 1995. Neuromagnetic fields of the brain evoked by voluntary movement and electrical stimulation of the index finger. Brain Res. 682 (1–2), 22–28.
Kuhn, A.A., 2004. Event-related beta desynchronization in human subthalamic nucleus correlates with motor performance. Brain 127 (4), 735–746.
Labyt, E., et al., 2003. Changes in oscillatory cortical activity related to a visuomotor task in young and elderly healthy subjects. Clin. Neurophysiol. 114 (6), 1153–1166.
Lange, R., et al., 2001. Passive finger movement evoked fields in magnetoencephalography. Exp. Brain Res. 136 (2), 194–199.
Mattay, V.S., et al., 2002. Neurophysiological correlates of age-related changes in human motor function. Neurology 58 (4), 630–635.
Muthukumaraswamy, S.D., 2011. Temporal dynamics of primary motor cortex gamma oscillation amplitude and piper corticomuscular coherence changes during motor control. Exp. Brain Res. 212 (4), 623–633.
Muthukumaraswamy, S.D., Singh, K.D., 2008. Spatiotemporal frequency tuning of BOLD and gamma band MEG responses compared in primary visual cortex. Neuroimage 40 (4), 1552–1560.
Muthukumaraswamy, S.D., et al., 2009. Resting GABA concentration predicts peak gamma frequency and fMRI amplitude in response to visual stimulation in humans. Proc. Natl. Acad. Sci. U. S. A. 106 (20), 8356–8361.
Muthukumaraswamy, S.D., et al., 2013. The effects of elevated endogenous GABA levels on movement-related network oscillations. Neuroimage 66, 36–41.
Nagamine, T., et al., 1996. Movement-related slow cortical magnetic fields and changes of spontaneous MEG- and EEG-brain rhythms. Electroencephalogr. Clin. Neurophysiol. 99 (3), 274–286.
Oishi, M., et al., 2004. Cortical activation in area 3b related to finger movement: an MEG study. Neuroreport 15 (1), 57–62.
Parkkonen, E., et al., 2015. Modulation of the ~20-Hz motor-cortex rhythm to passive movement and tactile stimulation. Brain Behav. 5 (5) e00328.
Pfurtscheller, G., 2001. Functional brain imaging based on ERD/ERS. Vis. Res. 41 (10–11), 1257–1260.
Pfurtscheller, G., Andrew, C., 1999. Event-Related changes of band power and coherence: methodology and interpretation. J. Clin. Neurophysiol. 16 (6), 512–519.
Pfurtscheller, G., Lopes da Silva, F.H., 1999. Event-related EEG/MEG synchronization and desynchronization: basic principles. Clin. Neurophysiol. 110 (11), 1842–1857.
Pfurtscheller, G., Neuper, C., 1997. Motor imagery activates primary sensorimotor area in humans. Neurosci. Lett. 239 (2–3), 65–68.
Pfurtscheller, G., Solis-Escalante, T., 2009. Could the beta rebound in the EEG be suitable to realize a "brain switch"? Clin. Neurophysiol. 120 (1), 24–29.
Pfurtscheller, G., Flotzinger, D., Neuper, C., 1994. Differentiation between finger, toe and tongue movement in man based on 40 Hz EEG. Electroencephalogr. Clin. Neurophysiol. 90 (6), 456–460.
Pfurtscheller, G., Stancak Jr., A., Neuper, C., 1996. Post-movement beta synchronization. A correlate of an idling motor area? Electroencephalogr. Clin. Neurophysiol. 98 (4), 281–293.
Pfurtscheller, G., Stancak Jr., A., Neuper, C., 1996. Event-related synchronization (ERS) in the alpha band–an electrophysiological correlate of cortical idling: a review. Int. J. Psychophysiol. 24 (1–2), 39–46.
Pfurtscheller, G., et al., 1997. Foot and hand area mu rhythms. Int. J. Psychophysiol. 26 (1–3), 121–135.
Pfurtscheller, G., et al., 1999. Visually guided motor imagery activates sensorimotor areas in humans. Neurosci. Lett. 269 (3), 153–156.
Pfurtscheller, G., et al., 2005. Beta rebound after different types of motor imagery in man. Neurosci. Lett. 378 (3), 156–159.
Piitulainen, H., et al., 2013. Corticokinematic coherence during active and passive finger movements. Neuroscience 238, 361–370.
Piitulainen, H., et al., 2018. Cortical proprioceptive processing is altered by aging. Front. Aging Neurosci. 10, 147.
Rossini, P.M., et al., 2007. Clinical neurophysiology of aging brain: from normal aging to neurodegeneration. Prog. Neurobiol. 83 (6), 375–400.
Rossiter, H.E., et al., 2014. Beta oscillations reflect changes in motor cortex inhibition in healthy ageing. Neuroimage 91, 360–365.
Sallard, E., et al., 2016. Age-related changes in post-movement beta synchronization during a selective inhibition task. Exp. Brain Res. 234 (12), 3543–3553.

Schmiedt-Fehr, C., et al., 2016. Aging differentially affects alpha and beta sensorimotor rhythms in a go/nogo task. Clin. Neurophysiol. 127 (10), 3234–3242.
Shafto, M.A., et al., 2014. The Cambridge Centre for Ageing and Neuroscience (Cam-CAN) study protocol: a cross-sectional, lifespan, multidisciplinary examination of healthy cognitive ageing. BMC Neurol. 14.
Szurhaj, W., et al., 2006. Relationship between intracerebral gamma oscillations and slow potentials in the human sensorimotor cortex. Eur. J. Neurosci. 24 (3), 947–954.
Taulu, S., Simola, J., 2006. Spatiotemporal signal space separation method for rejecting nearby interference in MEG measurements. Phys. Med. Biol. 51 (7), 1759–1768.
Taylor, J.R., et al., 2017. The Cambridge Centre for Ageing and Neuroscience (Cam-CAN) data repository: structural and functional MRI, MEG, and cognitive data from a cross-sectional adult lifespan sample. Neuroimage 144 (Pt B), 262–269.
Toledo, D.R., et al., 2016. Age-related differences in EEG beta activity during an assessment of ankle proprioception. Neurosci. Lett. 622, 1–5.
Toledo, D.R., et al., 2016. Cortical correlates of response time slowing in older adults: ERP and ERD/ERS analyses during passive ankle movement. Clin. Neurophysiol. 127 (1), 655–663.
Vallesi, A., et al., 2010. Age effects on the asymmetry of the motor system: evidence from cortical oscillatory activity. Biol. Psychol. 85 (2), 213–218.
Van Essen, D.C., et al., 2013. The Wu-Minn human connectome Project: an overview. Neuroimage 80, 62–79.
Woldag, H., et al., 2003. Cortical neuromagnetic fields evoked by voluntary and passive hand movements in healthy adults. J. Clin. Neurophysiol. 20 (2), 94–101.
Yordanova, J., et al., 2004. Sensorimotor slowing with ageing is mediated by a functional dysregulation of motor-generation processes: evidence from high-resolution event-related potentials. Brain 127, 351–362.